



Study on feasibility of producing an amorphous surface layer of $\text{Fe}_{49}\text{Cr}_{18}\text{Mo}_7\text{B}_{16}\text{C}_4\text{Nb}_3$ by pulsed Nd:YAG laser surface melting

Reza Mojaver^a, Faezeh Mojtahedi^b, Hamid Reza Shahverdi^{b,*}, Mohammad Javad Torkamany^c

^a Office of Applied Researches and Technology, Tarbiat Modares University, P.O. Box 14115-143, Tehran, Iran

^b Department of Materials Engineering, Tarbiat Modares University, P.O. Box 14115-143, Tehran, Iran

^c Iranian National Center for Laser Science and Technology, P.O. Box 14665-576, Tehran, Iran

ARTICLE INFO

Article history:

Received 5 June 2012

Received in revised form 3 September 2012

Accepted 30 September 2012

Available online 8 October 2012

Keywords:

Amorphous
Laser surface melting
Pulsed Nd:YAG laser
Fe-based glass former

ABSTRACT

This work aims to investigate whether an amorphous surface layer can be obtained when as-cast $\text{Fe}_{49}\text{Cr}_{18}\text{Mo}_7\text{B}_{16}\text{C}_4\text{Nb}_3$ alloy is submitted to pulsed Nd:YAG laser surface melting. The experiments were conducted in the various laser scanning speeds. The microstructures of laser treated zones were investigated by X-ray diffraction XRD and Field Emission Scanning Electron Microscope (FESEM) and their microhardness were measured, too. The chemical composition of different points of each sample was analyzed by energy-dispersive X-ray spectroscopy EDS. Although the estimated cooling rates in surface layers were higher than the required cooling rate to achieve full amorphization, but the present experiments were unable to retain complete glassy microstructure on surface and a mixture of amorphous (low volume fraction) and ultrafine grained phases were produced in surface of samples. Based on the findings, it was understood that the overlapping of successive pulses and element redistributions occurred in pulsed laser melting could severely restrict amorphization. The influence of laser scan speed and laser power on heat input, melting ratio, compositional changes and cracking in laser treated zone were discussed separately. It is suggested that the limited range of laser variables in pulsed Nd:YAG laser melting may help to produce a sound amorphous phase of as-cast $\text{Fe}_{49}\text{Cr}_{18}\text{Mo}_7\text{B}_{16}\text{C}_4\text{Nb}_3$ alloy.

© 2012 Elsevier B.V. All rights reserved.

1. Introduction

The amorphous alloys usually have the high hardness, high wear and corrosion resistance which make them excellent in their surface properties [1–4]. Among the metallic glass formers, Fe-based alloys are attractive because of their low cost [4,5]. So, during two last decades, many studies on the glass transition and crystallization process, structure, physical properties and corrosion behavior of Fe-based metallic glass alloys have been conducted [6–11]. However, compared to other amorphous alloys like Zr- and Pd-based alloys, Fe-based amorphous alloys have a lower glass-forming ability (GFA). Consequently, the higher critical cooling rates are required for their amorphization [6,8,10–12], ranging from values around 10^2 K/s in comparison with values about 1–10 K/s for alloys with very good glass-forming ability [8]. This limitation has inspired some attempts to develop some new Fe bulk metallic glass alloys which have a larger supercooled liquid region and a higher GFA [10,11,13,14].

While the characteristics mentioned above provide a few limitations in producing Fe-based bulk metallic glass parts, for example

obtained thickness could not be more than a few millimeters [8], but these alloys are expected to easily vitrify in forms of atomized powders and surface layers where production routes of them are associated with very high cooling rates. Amorphous layers of a few Fe system alloys might be obtained by different techniques including high velocity oxy-fuel, air plasma spraying [15] and these layers in different states, fully or partly amorphous or nano-grain sized microstructures (resulted from devitrifying-heat treatment) have even been entered in market [16].

In laser surface treatment LST (laser melting\alloying\cladding), a high energy laser beam can be irradiated on the surface of a crystalline bulk in a very short time by laser scanning at high speeds which could afford the cooling rates exactly in the bounds of the quench rates necessary for vitrification and nano-crystallization [17–22]. On the other hand, from the literature it can be found that not all attempts to provide an amorphous layer on metallic bases by laser surface treatment were successful [23–27]. The main reasons for the failure were explained as: (1) the redistribution of elements in weld metal [24,25]; (2) devitrification resulted from the reheating cycles induced by the successive laser tracks [20,21,23,26]; (3) epitaxial solidification which favors the crystal growth [18]; (4) inter-diffusion or dilution of some phases of substrate in the layer [24,25]. As well, contributions of some parameters of LST including laser scan speed, laser power [24–27], overlapping [21,23] and

* Corresponding author. Tel.: +98 21 82893307; fax: +98 21 82883101.
E-mail address: shahverdi@modares.ac.ir (H.R. Shahverdi).

Table 1
Chemical composition of as-cast alloy.

Elements	Fe	Cr	Mo	C	B	Nb
wt%	57	19	14	2	3.5	4.5

multi-track scanning [25] on surface amorphization have been investigated.

Generally speaking, it could be inferred that in order to gain an amorphous layer by LST, the criterion of cooling rate is not sufficient and all involving parameters in complicated reactions of laser processing and metallic glass formation should be considered. This fact might become more importance in pulse laser melting PLM where more variables like pulse shaping, pulse energy, pulse duration and frequency inevitably complicate the operation [28,29]. On the other hand, in pulsed laser melting coupling the high peak power with overlapping pulses produce a good melting ratio, a high cooling rate and a low heat input than those of the continuous wave laser melting that makes it theoretically a good tool for producing an amorphous layer [30].

$\text{Fe}_{52-x}\text{Cr}_{18}\text{Mo}_7\text{B}_{16}\text{C}_4\text{Nb}_x$ (at %) alloys are a group of Fe-based metallic glass alloys which glass forming ability and corrosion behaviors of their amorphous bulk in different amounts of Nb have earlier been studied [31–34]. In present study, the feasibility of producing an amorphous layer on surface of the as-cast $\text{Fe}_{49}\text{Cr}_{18}\text{Mo}_7\text{B}_{16}\text{C}_4\text{Nb}_3$ by pulsed laser melting in different scan speeds has been investigated and it has been aimed at correlating pulsed laser parameters with surface microstructure.

2. Experimental

Multicomponent alloy with nominal composition of $\text{Fe}_{49}\text{Cr}_{18}\text{Mo}_7\text{B}_{16}\text{C}_4\text{Nb}_3$ (at%) was prepared. The high purity materials Cr (>99.9 wt%), Mo (>99.9 wt%), C (>99.5 wt%), Nb (>99.9 wt%) and B (>99.9 wt%) as well as pre-alloyed Fe–C were selected and melted in a vacuum induction furnace. The melt was poured into a permanent mold. The chemical composition of the ingot was investigated by inductively coupled plasma spectrometry (ICP) and the result is given in Table 1. A few plates with dimensions of 30 mm × 60 mm × 2 mm were cut from the ingot for laser processing. Before laser treatment the surface of the plates were ground and cleaned with acetone to remove impurities.

A pulsed Nd:YAG laser Model IQL-10 with a maximum mean laser power of 400 W was used as laser source for the experiments. More detail about the laser processing setup can be found elsewhere [30]. The treatments were carried out using pulsed laser with the focused beam diameter of 0.9 mm, pulse frequency of 40 Hz and pulse duration of 2 ms at various scanning speeds of 4, 5, 6.67 and 8 mm/s, A1–A4. A summary of these parameters is shown in Table 2. These conditions were chosen in the way that laser processing occurred in conduction mode, but with a little change in parameters, it might change to keyhole mode. During the process, the surface was protected by pure Ar gas emerged coaxially with the laser beam. Two types of samples were prepared: single track treated plates which were used for study on microstructures by

Table 2
Summary of pulsed laser melting.

Sample name	Average power (W)	Frequency (Hz)	Pulse duration (ms)	Beam diameter (mm)	Laser scan speed (mm/s)	Overlapping factor (%)	Accumulative overlapping index F	Effective peak power density (KW/mm ²)
A1	170	40	2	0.9	4	89	6.5	12.363
A2	170	40	2	0.9	5	86	5.3	10.08
A3	170	40	2	0.9	6.67	81	4.1	7.795
A4	170	40	2	0.9	8	78	3.5	6.657

D, 1.2 mm; pulse peak power, 2.125 KW.

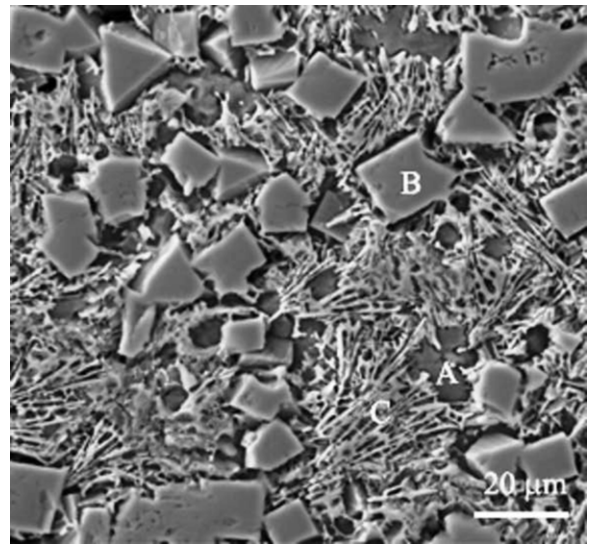


Fig. 1. Back scattered SEM image of microstructure of the as-cast alloy.

Field Emission Scanning Electron Microscope (FESEM) and multi track treated plates which were used for X-ray diffraction (XRD) studying, using Co $K\alpha$ radiation. In the later case, the treatment was conducted in the way that percentage of overlapping between neighboring tracks was less than 10%.

The elements distribution in parent alloy and remelted pools was analyzed by energy-dispersive X-ray spectroscopy (EDS) after Ar-ion etching (Ar-ion accelerating voltage-3 kV, ion current 30 μA , diameter and raster of ion beam were 120 μm and 1 mm, respectively and etching time was 240 s). The sample surface layer was removed about 20 nm in thickness during cleaning procedure which was necessary for appropriate light elements analyses, mainly B and C. EDS analyses were done at both accelerating voltages of the electron beam of 10 kV and 30 kV. The results showed that distribution of B, C and Nb were much clear in 10 kV.

In addition, the Vickers microhardness profiles were extracted from cross-sections of the processed samples by applying a 200 gf load for 15 s. The reported dates are the average of nine measurements for each sample.

3. Results and discussion

3.1. Microstructure of base metal

Fig. 1 shows the microstructure of parent alloy. Investigation by XRD, EDS and X-ray map showed that five phases could be identified in the parent alloy, labeled A–E. The phases called D and E which are distributed in matrix of phase C are very small ones and they are not visible at the image represented in Fig. 1. So, they are not labeled on this figure. Authors could not find any references in literature to characterize phases certainly. However, according to compositions (represented at Table 3) and XRD of parent alloy (Fig. 2) and by considering the average atomic weight and

Download English Version:

<https://daneshyari.com/en/article/5354025>

Download Persian Version:

<https://daneshyari.com/article/5354025>

[Daneshyari.com](https://daneshyari.com)